Constraints on anomalous QGC's in e^+e^- interactions from 183 to 209 GeV

A. Heister, S. Schael, R. Barate, R. Bruneliere, I. de Bonis, D. Decamp, C. Goy, S. Jezequel, J.P. Lees, F. Martin, et al.

To cite this version:

A. Heister, S. Schael, R. Barate, R. Bruneliere, I. de Bonis, et al.. Constraints on anomalous QGC's in e^+e^- interactions from 183 to 209 GeV. Physics Letters B, Elsevier, 2004, 602, pp.31-40. 10.1016/j.physletb.2004.09.041 . in2p3-00021735

HAL Id: in2p3-00021735

http://hal.in2p3.fr/in2p3-00021735

Submitted on 27 Apr 2004

ORGANISATION EUROPÉENNE POUR LA RECHERCHE NUCLÉAIRE (CERN)
Laboratoire Européen pour la Physique des Particules

CERN-PH-EP/04-001
05-Jan-2004

Constraints on anomalous QGC's in e^+e^- interactions from 183 to 209 GeV

The ALEPH Collaboration*)

Abstract

The acoplanar photon pairs produced in the reaction $e^+e^- \rightarrow \nu\bar{\nu}\gamma\gamma$ are analysed in the $700\,\mathrm{pb}^{-1}$ of data collected by the ALEPH detector at centre-of-mass energies between 183 and 209 GeV. No deviation from the Standard Model predictions is seen in any of the distributions examined. The resulting 95% C.L. limits set on the anomalous QGC's, a_0^Z, a_c^Z, a_0^W and a_c^W, are

$$\begin{array}{lll} -0.012\,\mathrm{GeV}^{-2} & < a_0^Z/\Lambda^2 & < +0.019\,\mathrm{GeV}^{-2}, \\ -0.041\,\mathrm{GeV}^{-2} & < a_c^Z/\Lambda^2 & < +0.044\,\mathrm{GeV}^{-2}, \\ -0.060\,\mathrm{GeV}^{-2} & < a_0^W/\Lambda^2 & < +0.055\,\mathrm{GeV}^{-2}, \\ -0.099\,\mathrm{GeV}^{-2} & < a_c^W/\Lambda^2 & < +0.093\,\mathrm{GeV}^{-2}, \end{array}$$

where Λ is the energy scale of the new Physics responsible for the anomalous couplings.

Submitted to Physics Letters B

---

*) See next pages for the list of authors

The ALEPH Collaboration

A. Heister, S. Schael

Physikalisches Institut das RWTH-Aachen, D-52056 Aachen, Germany

R. Barate, R. Brunelière, I. De Bonis, D. Decamp, C. Goy, S. Jézéquel, J.-P. Lees, F. Martin, E. Merle, M.-N. Minard, B. Pietrzyk, B. Trocmé

Laboratoire de Physique des Particules (LAPP), IN^{2}P^3-CNRS, F-74019 Annecy-le-Vieux Cedex, France

S. Bravo, M.P. Casado, M. Chmeissani, J.M. Crespo, E. Fernandez, M. Fernandez-Bosman, Ll. Garrido,[15] M. Martinez, A. Pacheco, H. Ruiz

Institut de Física d'Altes Energies, Universitat Autònoma de Barcelona, E-08193 Bellaterra (Barcelona), Spain[7]

A. Colaleo, D. Creanza, N. De Filippis, M. de Palma, G. Iaselli, G. Maggi, M. Maggi, S. Nuzzo, A. Ranieri, G. Raso,[24] F. Ruggieri, G. Selvaggi, L. Silvestris, P. Tempesta, A. Tricomi,[3] G. Zito

Dipartimento di Fisica, INFN Sezione di Bari, I-70126 Bari, Italy

X. Huang, J. Lin, Q. Ouyang, T. Wang, Y. Xie, R. Xu, S. Xue, J. Zhang, L. Zhang, W. Zhao

Institute of High Energy Physics, Academia Sinica, Beijing, The People's Republic of China[8]

D. Abbaneo, T. Barklow,[26] O. Buchmüller,[26] M. Cattaneo, B. Clerbaux,[23] H. Drevermann, R.W. Forty, M. Frank, F. Gianotti, J.B. Hansen, J. Harvey, D.E. Hutchcroft,[30], P. Janot, B. Jost, M. Kado,[2] P. Mato, A. Moutoussi, F. Ranjard, L. Rolandi, D. Schlatter, G. Sguazzoni, F. Teubert, A. Valassi, I. Videau

European Laboratory for Particle Physics (CERN), CH-1211 Geneva 23, Switzerland

F. Badaud, S. Dessagne, A. Falvard,[20] D. Fayolle, P. Gay, J. Jousset, B. Michel, S. Monteil, D. Pallin, J.M. Pascolo, P. Perret

Laboratoire de Physique Corpusculaire, Université Blaise Pascal, IN^{2}P^3-CNRS, Clermont-Ferrand, F-63177 Aubière, France

J.D. Hansen, J.R. Hansen, P.H. Hansen, A.C. Kraan, B.S. Nilsson

Niels Bohr Institute, 2100 Copenhagen, DK-Denmark[9]

A. Kyriakis, C. Markou, E. Simopoulou, A. Vayaki, K. Zachariadou

Nuclear Research Center Demokritos (NRCD), GR-15310 Attiki, Greece

A. Blondel,[12] J.-C. Brient, F. Machefert, A. Rougé, H. Videau

Laoratoire Leprince-Ringuet, Ecole Polytechnique, IN^{2}P^3-CNRS, F-91128 Palaiseau Cedex, France

V. Ciulli, E. Focardi, G. Parrini

Dipartimento di Fisica, Università di Firenze, INFN Sezione di Firenze, I-50125 Firenze, Italy

A. Antonelli, M. Antonelli, G. Bencivenni, F. Bossi, G. Capon, F. Cerutti, V. Chiarella, P. Laurelli, G. Mannocchi,[5] G.P. Murtas, L. Passalacqua

Laboratori Nazionali dell'INFN (LNF-INFN), I-00044 Frascati, Italy

J. Kennedy, J.G. Lynch, P. Negus, V. O'Shea, A.S. Thompson

Department of Physics and Astronomy, University of Glasgow, Glasgow G12 8QQ,United Kingdom[10]

S. Wasserbaech

Utah Valley State College, Orem, UT 84058, U.S.A.

R. Cavanaugh,[4] S. Dhamotharan,[21] C. Geweniger, P. Hanke, V. Hepp, E.E. Kluge, A. Putzer, H. Stenzel,

K. Tittel, M. Wunsch[19]

Kirchhoff-Institut für Physik, Universität Heidelberg, D-69120 Heidelberg, Germany[16]

R. Beuselinck, W. Cameron, G. Davies, P.J. Dornan, M. Girone,[1] R.D. Hill, N. Marinelli, J. Nowell, S.A. Rutherford, J.K. Sedgbeer, J.C. Thompson,[14] R. White

Department of Physics, Imperial College, London SW7 2BZ, United Kingdom[10]

V.M. Ghete, P. Girtler, E. Kneringer, D. Kuhn, G. Rudolph

Institut für Experimentalphysik, Universität Innsbruck, A-6020 Innsbruck, Austria[18]

E. Bouhova-Thacker, C.K. Bowdery, D.P. Clarke, G. Ellis, A.J. Finch, F. Foster, G. Hughes, R.W.L. Jones, M.R. Pearson, N.A. Robertson, M. Smizanska

Department of Physics, University of Lancaster, Lancaster LA1 4YB, United Kingdom[10]

O. van der Aa, C. Delaere,[28] G.Leibenguth,[31] V. Lemaitre[29]

Institut de Physique Nucléaire, Département de Physique, Université Catholique de Louvain, 1348 Louvain-la-Neuve, Belgium

U. Blumenschein, F. Hölldorfer, K. Jakobs, F. Kayser, K. Kleinknecht, A.-S. Müller, B. Renk, H.-G. Sander, S. Schmeling, H. Wachsmuth, C. Zeitnitz, T. Ziegler

Institut für Physik, Universität Mainz, D-55099 Mainz, Germany[16]

A. Bonissent, P. Coyle, C. Curtil, A. Ealet, D. Fouchez, P. Payre, A. Tilquin

Centre de Physique des Particules de Marseille, Univ Méditerranée, IN^{2}P^{3}-CNRS, F-13288 Marseille, France

F. Ragusa

Dipartimento di Fisica, Università di Milano e INFN Sezione di Milano, I-20133 Milano, Italy.

A. David, H. Dietl,[32] G. Ganis,[27] K. Hüttmann, G. Lütjens, W. Männer[32], H.-G. Moser, R. Settles, M. Villegas, G. Wolf

Max-Planck-Institut für Physik, Werner-Heisenberg-Institut, D-80805 München, Germany[16]

J. Boucrot, O. Callot, M. Davier, L. Duflot, J.-F. Grivaz, Ph. Heusse, A. Jacholkowska,[6] L. Serin, J.-J. Veillet

Laboratoire de l'Accélérateur Linéaire, Université de Paris-Sud, IN^{2}P^{3}-CNRS, F-91898 Orsay Cedex, France

P. Azzurri, G. Bagliesi, T. Boccali, L. Foà, A. Giammanco, A. Giassi, F. Ligabue, A. Messineo, F. Palla, G. Sanguinetti, A. Sciabà, P. Spagnolo, R. Tenchini, A. Venturi, P.G. Verdini

Dipartimento di Fisica dell'Università, INFN Sezione di Pisa, e Scuola Normale Superiore, I-56010 Pisa, Italy

O. Awunor, G.A. Blair, G. Cowan, A. Garcia-Bellido, M.G. Green, T. Medcalf, A. Misiejuk, J.A. Strong, P. Teixeira-Dias

Department of Physics, Royal Holloway & Bedford New College, University of London, Egham, Surrey TW20 OEX, United Kingdom[10]

R.W. Clifft, T.R. Edgecock, P.R. Norton, I.R. Tomalin, J.J. Ward

Particle Physics Dept., Rutherford Appleton Laboratory, Chilton, Didcot, Oxon OX11 OQX, United Kingdom[10]

B. Bloch-Devaux, D. Boumediene, P. Colas, B. Fabbro, E. Lançon, M.-C. Lemaire, E. Locci, P. Perez, J. Rander, B. Tuchming, B. Vallage

CEA, DAPNIA/Service de Physique des Particules, CE-Saclay, F-91191 Gif-sur-Yvette Cedex, France[17]

A.M. Litke, G. Taylor

Institute for Particle Physics, University of California at Santa Cruz, Santa Cruz, CA 95064, USA[22]

C.N. Booth, S. Cartwright, F. Combley,[25] P.N. Hodgson, M. Lehto, L.F. Thompson

Department of Physics, University of Sheffield, Sheffield S3 7RH, United Kingdom[10]

A. Böhrer, S. Brandt, C. Grupen, J. Hess, A. Ngac, G. Prange

Fachbereich Physik, Universität Siegen, D-57068 Siegen, Germany[16]

C. Borean, G. Giannini

Dipartimento di Fisica, Università di Trieste e INFN Sezione di Trieste, I-34127 Trieste, Italy

H. He, J. Putz, J. Rothberg

Experimental Elementary Particle Physics, University of Washington, Seattle, WA 98195 U.S.A.

S.R. Armstrong, K. Berkelman, K. Cranmer, D.P.S. Ferguson, Y. Gao,[13] S. González, O.J. Hayes, H. Hu, S. Jin, J. Kile, P.A. McNamara III, J. Nielsen, Y.B. Pan, J.H. von Wimmersperg-Toeller, W. Wiedenmann, J. Wu, Sau Lan Wu, X. Wu, G. Zobernig

Department of Physics, University of Wisconsin, Madison, WI 53706, USA[11]

G. Dissertori

Institute for Particle Physics, ETH Hönggerberg, 8093 Zürich, Switzerland.

---

[1] Also at CERN, 1211 Geneva 23, Switzerland.

[2] Now at Fermilab, PO Box 500, MS 352, Batavia, IL 60510, USA

[3] Also at Dipartimento di Fisica di Catania and INFN Sezione di Catania, 95129 Catania, Italy.

[4] Now at University of Florida, Department of Physics, Gainesville, Florida 32611-8440, USA

[5] Also IFSI sezione di Torino, CNR, Italy.

[6] Also at Groupe d'Astroparticules de Montpellier, Université de Montpellier II, 34095, Montpellier, France.

[7] Supported by CICYT, Spain.

[8] Supported by the National Science Foundation of China.

[9] Supported by the Danish Natural Science Research Council.

[10] Supported by the UK Particle Physics and Astronomy Research Council.

[11] Supported by the US Department of Energy, grant DE-FG0295-ER40896.

[12] Now at Departement de Physique Corpusculaire, Université de Genève, 1211 Genève 4, Switzerland.

[13] Also at Department of Physics, Tsinghua University, Beijing, The People's Republic of China.

[14] Supported by the Leverhulme Trust.

[15] Permanent address: Universitat de Barcelona, 08208 Barcelona, Spain.

[16] Supported by Bundesministerium für Bildung und Forschung, Germany.

[17] Supported by the Direction des Sciences de la Matière, C.E.A.

[18] Supported by the Austrian Ministry for Science and Transport.

[19] Now at SAP AG, 69185 Walldorf, Germany

[20] Now at Groupe d' Astroparticules de Montpellier, Université de Montpellier II, 34095 Montpellier, France.

[21] Now at BNP Paribas, 60325 Frankfurt am Mainz, Germany

[22] Supported by the US Department of Energy, grant DE-FG03-92ER40689.

[23] Now at Institut Inter-universitaire des hautes Energies (IIHE), CP 230, Université Libre de Bruxelles, 1050 Bruxelles, Belgique

[24] Also at Dipartimento di Fisica e Tecnologie Relative, Università di Palermo, Palermo, Italy.

[25] Deceased.

[26] Now at SLAC, Stanford, CA 94309, U.S.A

[27] Now at IWR, Forschungzentrum Karlsruhe, Postfach 3640, 76021 Karlsruhe, Germany

[28] Research Fellow of the Belgium FNRS

[29] Research Associate of the Belgium FNRS

[30] Now at Liverpool University, Liverpool L69 7ZE, United Kingdom

[31] Supported by the Federal Office for Scientific, Technical and Cultural Affairs through the Interuniversity Attraction Pole P5/27

[32] Now at Henryk Niewodnicznski Institute of Nuclear Physics, Polish Academy of Sciences, Cracow, Poland

1 Introduction

Multiphoton production has been already investigated with the ALEPH detector to search for physics beyond the Standard Model [1]. In this letter, acoplanar photon pairs from the reaction $e^+e^- \to \nu\bar{\nu}\gamma\gamma$ are used to set limits on anomalous quartic gauge couplings.

Quartic gauge couplings (QGC's) between the electroweak vector bosons are predicted by the Standard Model (SM), as a consequence of the SU(2) × U(1) non-Abelian gauge structure. The SM QGC contributions are unobservably small at LEP2 energies. For example the contribution of the $WW\gamma\gamma$ vertex (Fig. 1) to the $e^+e^- \to \nu\bar{\nu}\gamma\gamma$ process is only a few fb [2, 3]. The $ZZ\gamma\gamma$ vertex is absent in the SM at tree level. Therefore evidence of QGC's at LEP2 would be an indication of new physics.

The values of the QGC's depend strongly on the electroweak symmetry breaking mechanism. Several alternatives to the SM predict anomalous QGC's without altering the SM values of the triple gauge couplings [4, 5].

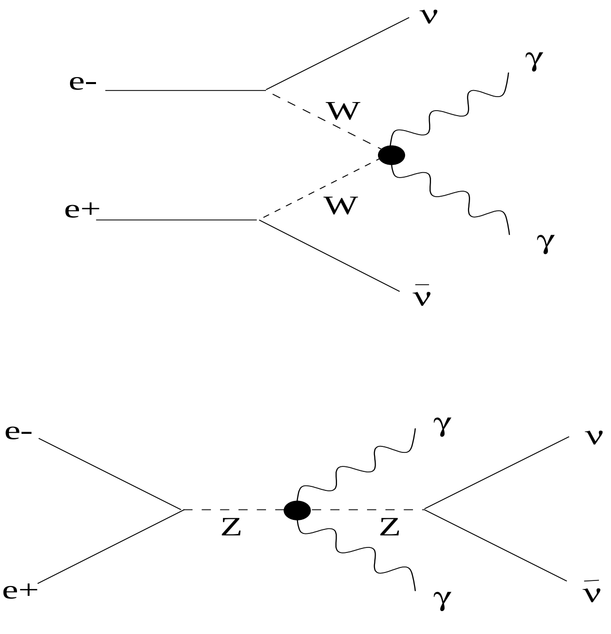

Figure 1: *Diagrams with quartic gauge couplings contributing to the* $e^+e^- \to \nu\bar{\nu}\gamma\gamma$ *channel.*

The parametrization of QGC's adopted in this paper follows the convention of Ref. [2]. The relevant C, P and CP conserving anomalous QGC contributions, not related to a TGC counterpart, are described by two additional dimension-six terms in the Lagrangian [3]:

$$\begin{aligned} L_6^0 &= -\frac{e^2}{16}\,\frac{a_0}{\Lambda^2}\,F^{\mu\nu}F_{\mu\nu}\,\overrightarrow{W^{\alpha}}\cdot\overrightarrow{W_{\alpha}}, \\ L_6^c &= -\frac{e^2}{16}\,\frac{a_c}{\Lambda^2}\,F^{\mu\alpha}F_{\mu\beta}\,\overrightarrow{W^{\beta}}\cdot\overrightarrow{W_{\alpha}} \end{aligned}$$

with usual notations for the electromagnetic and weak fields, and where Λ represents the scale of the new physics responsible for the anomalous contributions. Both a_0 and a_c are equal to zero in the Standard Model. In the following, the two sets of couplings, $(a_0^\mathrm{W}, a_\mathrm{c}^\mathrm{W})$ and $(a_0^\mathrm{Z}, a_\mathrm{c}^\mathrm{Z})$, are assumed to be independent, as suggested in Ref. [6].

2 The ALEPH detector and event selection

2.1 The ALEPH detector

The ALEPH detector and its performance are described in detail in [7] and [8]. The analysis presented here depends mainly on the performance of the electromagnetic calorimeter (ECAL). The ECAL is a lead/wire chamber sampling calorimeter of 22 radiation length thickness. It consists of 36 modules, twelve in the barrel and twelve in each endcap, which provide coverage in the angular range $|\cos\theta| < 0.98$. The insensitive region between modules represents 2% of the barrel and 6% of the endcap areas. Cathode pads associated with each layer of the wire chambers are connected to form projective towers, each subtending approximately $0.9^\circ \times 0.9^\circ$, read out in three segments in depth ("storeys"). This high granularity provides excellent identification of photons. The energy calibration of the ECAL is obtained from Bhabha events, $\mathrm{e^+e^-} \rightarrow \gamma\gamma$ events and events from two-photon interactions, $\gamma\gamma \rightarrow \mathrm{e^+e^-}$. The energy resolution for isolated photons is $\sigma(E)/E = 0.18/\sqrt{E} + 0.009$ (E in GeV). The ECAL also provides a measurement of the event time t_0 relative to the beam crossing with a resolution better than 15 ns for showers with energy greater than 1 GeV.

The hadron calorimeter (HCAL) and the luminosity calorimeters extend the coverage to 34 mrad from the beam axis. Together with external muon chambers, they are used in this analysis mainly to veto events in which photons are accompanied by other energetic particles. The tracking system provides efficient reconstruction of isolated charged particles in the angular range $|\cos\theta| < 0.95$. Photon candidates are identified by an algorithm [8] which searches for local energy maxima within clusters of ECAL storeys. The trigger most relevant for photon events is the neutral-energy trigger with a threshold of 1 GeV (2.3 GeV) in any ECAL barrel (endcap) module. The trigger efficiency for the selections described below is estimated to be at least 99.8%.

The data have been collected at centre-of-mass energies between 183 and 209 GeV. Only runs during which all tracking devices and calorimeters were in standard working conditions are selected, corresponding to a total luminosity of 704.4 pb^{-1}.

2.2 Monte Carlo simulation

The KK generator version 4.15 [9] is used to simulate the SM processes for the reaction $\mathrm{e^+e^-} \rightarrow \nu\bar{\nu}\gamma\gamma(\gamma)$. It uses the YFS approach [10] to generate an arbitrary number of initial state photons. An independent generator, NUNUGPV [11], based on exact lowest order amplitudes for the production of up to three photons in the final state, modified for higher order QED effects using transverse momentum dependent structure functions, is used to reweight the events as a function of the anomalous couplings a_0 and a_c. The cross sections predicted by the two generators in the absence of anomalous couplings are consistent within 1% at LEP2 energies.

The simulations have been performed at eight centre of mass energies between 182.6 and 206.7 GeV, corresponding to the average energies of the data samples. For each energy, a sample of 10000 events has been generated and processed through the ALEPH simulation and reconstruction programs.

In the following sections, the missing mass ($\mathrm{M_{miss}}$) is used as a discriminant variable to set constraints on the anomalous couplings $a_0^{\mathrm{Z}}, a_0^{\mathrm{W}}$ and $a_{\mathrm{c}}^{\mathrm{Z}}, a_{\mathrm{c}}^{\mathrm{W}}$. The distribution of the missing mass is shown in Fig. 2 for the SM and for a few values of a_0^{Z} and $a_{\mathrm{c}}^{\mathrm{Z}}$. A larger sensitivity to the $\mathrm{ZZ}\gamma\gamma$ vertex is expected because of the resonant nature of the relevant graph in Fig. 1.

2.3 Selection of events with two acoplanar high transverse momentum photons

Only events with photons having a time measurement consistent with the beam crossing time, no reconstructed charged particle tracks and total photon energy $\sum E_\gamma < 0.5\sqrt{s}$ are considered. No more than one hit is allowed in the muon chambers, to eliminate background arising from off-momentum muons in the beam halo and cosmic rays. Beam-related background is suppressed by rejecting events with at least 0.5 GeV detected below 14° from the beam axis. Events with a photon acoplanarity above 5° are kept, to reject the events from the QED reaction $\mathrm{e^+e^-} \to \gamma\gamma(\gamma)$.

Events with two and only two photon candidates are considered. Both photons must fulfil the conditions

$$E_\gamma/\sqrt{s} > 0.025 \ , \ |\cos\theta_\gamma| < 0.94 \text{ and } p_{T\gamma}/E_{beam} > 0.05,$$

and the more energetic photon must have an energy larger than $0.2\sqrt{s}$.

The average reconstruction efficiency of events which fulfil the above cuts is 70.0±2.0%. In the data 30 events are found, whereas 36.2 are expected from SM contributions, as summarized in Table 1.

Figure 3 shows the distribution of the photon energy, of $|\cos\theta_\gamma|$ and of the missing mass for data, compared to the SM predictions from KK.

3 Results

3.1 Likelihood fit

For the $\mathrm{ZZ}\gamma\gamma$ vertex a 2-dimensional binned likelihood fit is performed on the $(\mathrm{M_{miss}}, \mathrm{E_\gamma})$ distribution, with 4 bins in $\mathrm{M_{miss}}$ as displayed on Fig.2 and 2 bins in $\mathrm{E_\gamma}$ as shown in Table 1. For the $\mathrm{WW}\gamma\gamma$ vertex only the $\mathrm{M_{miss}}$ distribution is used.

	All	High E_γ	Low E_γ
Data Events	30	10	20
Expected events (SM)	36.2	11.6	24.6
Expected events for $a_0^{\mathrm{Z}} = a_c^{\mathrm{Z}} = 300$	82.1	13.1	69.0

Table 1: *Number of events in the data, number of events expected from the SM, and number of events expected for $a_0^{\mathrm{Z}} = a_c^{\mathrm{Z}} = 300$. High E_γ : events for which the energy of the less energetic photon is $> 0.1\sqrt{s}$. Low E_γ : energy of the less energetic photon $< 0.1\sqrt{s}$. The new physics scale Λ is set to the mass of the W boson.*

The two pairs of QGC parameters, $(a_0^{\mathrm{Z}}, a_c^{\mathrm{Z}})$ and $(a_0^{\mathrm{W}}, a_c^{\mathrm{W}})$, are determined independently, setting the WW$\gamma\gamma$ (respectively ZZ$\gamma\gamma$) contribution to zero.

Figure 4 shows the -Δlog(L) curve corresponding to the fit of $a_0^{\mathrm{Z}}/\Lambda^2$ with a_c^{Z} set to zero, and the -Δlog(L) curve for the fit of $a_c^{\mathrm{Z}}/\Lambda^2$ with a_0^{Z} set to zero. Figure 5 shows the corresponding likelihood curves for $a_0^{\mathrm{W}}/\Lambda^2$ and $a_c^{\mathrm{W}}/\Lambda^2$.

Figure 6 shows the 68% and 95% confidence level contours in the $(a_0^{\mathrm{Z}}/\Lambda^2, a_c^{\mathrm{Z}}/\Lambda^2)$ and $(a_0^{\mathrm{W}}/\Lambda^2, a_c^{\mathrm{W}}/\Lambda^2)$ planes from a two-parameter fit. A weak correlation between the couplings is visible in both two-dimensional likelihood functions.

3.2 Systematic uncertainties

The contributions to the systematic uncertainty on the determination of the couplings are summarized in Table 2.

Table 2: *Contributions to the systematic uncertainty on the measurements of the couplings, in percent of the cross section. The statistical relative error on the measured cross section is 18%.*

Source of systematic uncertainty	Error (%)
Higher Order corrections	1.0
Weight calculation	5.0
Acceptance	1.0
Normalization	5.0
Energy scale	negligible
Background	negligible
Total	8.0

The effect of absence of higher order electroweak corrections in the NUNUGPV generator has been determined by the authors of Ref.[9] to be around 1 %. The theoretical error is dominated by the QGC reweighting procedure; this error has been estimated to be of the order of 5%. The acceptance is found to be stable within 1% when the couplings are varied. Taking into account the uncertainty on the inefficiency of the cut at 14° described in Section 2.3, that of the cut on the number of hits in the muon chambers and the 0.5%

uncertainty on the luminosity, the error on the normalization is estimated to be 5%. The contribution to the background from QED events with 3 or more photons is estimated by the GGGB program [12], to be less than 0.01 events.

The total systematic error of 8% is small with respect to the 18% statistical error on the measured cross section. Its contribution is convolved with the statistical component to extract the final 95% confidence level limits on the quartic gauge couplings; these limits are

$$\begin{array}{rl}
-0.012\ \mathrm{GeV}^{-2} < a_0^{\mathrm{Z}}/\Lambda^2 < 0.019\ \mathrm{GeV}^{-2} & \text{with } a_{\mathrm{c}}^{\mathrm{Z}} = 0, \\
-0.041\ \mathrm{GeV}^{-2} < a_{\mathrm{c}}^{\mathrm{Z}}/\Lambda^2 < 0.044\ \mathrm{GeV}^{-2} & \text{with } a_0^{\mathrm{Z}} = 0, \\
-0.060\ \mathrm{GeV}^{-2} < a_0^{\mathrm{W}}/\Lambda^2 < 0.055\ \mathrm{GeV}^{-2} & \text{with } a_{\mathrm{c}}^{\mathrm{W}} = 0, \\
-0.099\ \mathrm{GeV}^{-2} < a_{\mathrm{c}}^{\mathrm{W}}/\Lambda^2 < 0.093\ \mathrm{GeV}^{-2} & \text{with } a_0^{\mathrm{W}} = 0.
\end{array}$$

The limits from the 2-parameter fit are

$$\begin{array}{rl}
-0.020\ \mathrm{GeV}^{-2} < a_0^{\mathrm{Z}}/\Lambda^2 < 0.024\ \mathrm{GeV}^{-2} & , \\
-0.050\ \mathrm{GeV}^{-2} < a_{\mathrm{c}}^{\mathrm{Z}}/\Lambda^2 < 0.055\ \mathrm{GeV}^{-2} & , \\
-0.075\ \mathrm{GeV}^{-2} < a_0^{\mathrm{W}}/\Lambda^2 < 0.066\ \mathrm{GeV}^{-2} & , \\
-0.121\ \mathrm{GeV}^{-2} < a_{\mathrm{c}}^{\mathrm{W}}/\Lambda^2 < 0.116\ \mathrm{GeV}^{-2} & .
\end{array}$$

4 Conclusions

No evidence of anomalous quartic gauge couplings in the $\mathrm{ZZ}\gamma\gamma$ and $\mathrm{WW}\gamma\gamma$ processes has been found in the analysis of the $\mathrm{e}^+\mathrm{e}^- \to \nu\bar{\nu}\gamma\gamma$ reaction in a data sample taken at energies between 183 and 209 GeV with the ALEPH detector, corresponding to an integrated luminosity of 704.4 pb^{-1}.

The 95 % C.L. limits on the QGC parameters a_0/Λ^2 and a_c/Λ^2 are

$$\begin{array}{rl}
-0.012\ \mathrm{GeV}^{-2} < a_0^{\mathrm{Z}}/\Lambda^2 < 0.019\ \mathrm{GeV}^{-2} & \text{with } a_{\mathrm{c}}^{\mathrm{Z}} = 0, \\
-0.041\ \mathrm{GeV}^{-2} < a_{\mathrm{c}}^{\mathrm{Z}}/\Lambda^2 < 0.044\ \mathrm{GeV}^{-2} & \text{with } a_0^{\mathrm{Z}} = 0, \\
-0.060\ \mathrm{GeV}^{-2} < a_0^{\mathrm{W}}/\Lambda^2 < 0.055\ \mathrm{GeV}^{-2} & \text{with } a_{\mathrm{c}}^{\mathrm{W}} = 0, \\
-0.099\ \mathrm{GeV}^{-2} < a_{\mathrm{c}}^{\mathrm{W}}/\Lambda^2 < 0.093\ \mathrm{GeV}^{-2} & \text{with } a_0^{\mathrm{W}} = 0.
\end{array}$$

Constraints on these parameters have been set also by the OPAL collaboration [13] and by the L3 collaboration [14].

5 Acknowledgements

We thank and congratulate our colleagues in the CERN accelerator divisions for the successful operation of LEP2. We are indebted to the engineers and technicians in all our institutions for their contribution to the excellent performance of ALEPH. Those of us from non-member countries thank CERN for its hospitality and support.

References

[1] ALEPH Collaboration, *Single and multi-photon productions in* e^+e^- *collisions at* $\sqrt{s}$ *up to 209 GeV*, Eur. Phys. J. **C28** (2003) 1.

[2] G. Bélanger and F. Boudjema, Phys. Lett. **B288** (1992) 201.

[3] W.J. Stirling and A. Werthenbach, Eur. Phys. J. **C14** (2000) 103.

[4] R. Casalbuoni, S. de Curtis, D. Dominici and R. Gatto, Nucl. Phys. **B282** (1987) 235.

[5] A. Hill and J.J. van der Bij, Phys. Rev. **D36** (1987) 3463.

[6] G. Bélanger *et al.*, Eur. Phys. J. **C13** (2000) 283.

[7] ALEPH Collaboration, *ALEPH: A detector for electron-positron annihilations at LEP*, Nucl. Instrum. and Methods **A294** (1990) 121.

[8] ALEPH Collaboration, *Performance of the ALEPH detector at LEP*, Nucl. Instrum. and Methods **A360** (1995) 481.

[9] S. Jadach, B.F.L. Ward and Z. Wąs, Comput. Phys. Commun. **130** (2000) 260.

The above reference describes the KK generator, version 4.14. The version 4.15 used in this paper is a slightly modified version of 4.14 (Z.Wąs, private communication).

[10] D.R. Yennie, D.C. Frautschi and H. Suura, Annals of Physics **13** (1961) 379.

[11] G. Montagna *et al.*, Nucl. Phys. **B541** (1999) 31.
G. Montagna *et al.*, Phys.Lett **B515** (2001) 197.

[12] F.A. Berends and R. Kleiss, Nucl. Phys. **B186** (1981) 22.

[13] OPAL Collaboration, *A study of* $W^+W^-\gamma$ *Events at LEP* , CERN-EP/2003-043, July 2003, submitted to Phys. Lett. B.

[14] L3 Collaboration, *Study of the* $W^+W^-\gamma$ *Process and limits on Anomalous Quartic Gauge Boson Couplings at LEP* , Phys. Lett. **B527** (2002) 29.

L3 Collaboration, *The* $e^+e^- \rightarrow Z\gamma\gamma \rightarrow q\bar{q}\gamma\gamma$ *reaction at LEP and constraints on Anomalous Quartic Gauge Boson Couplings* , Phys. Lett. **B540** (2002) 43.

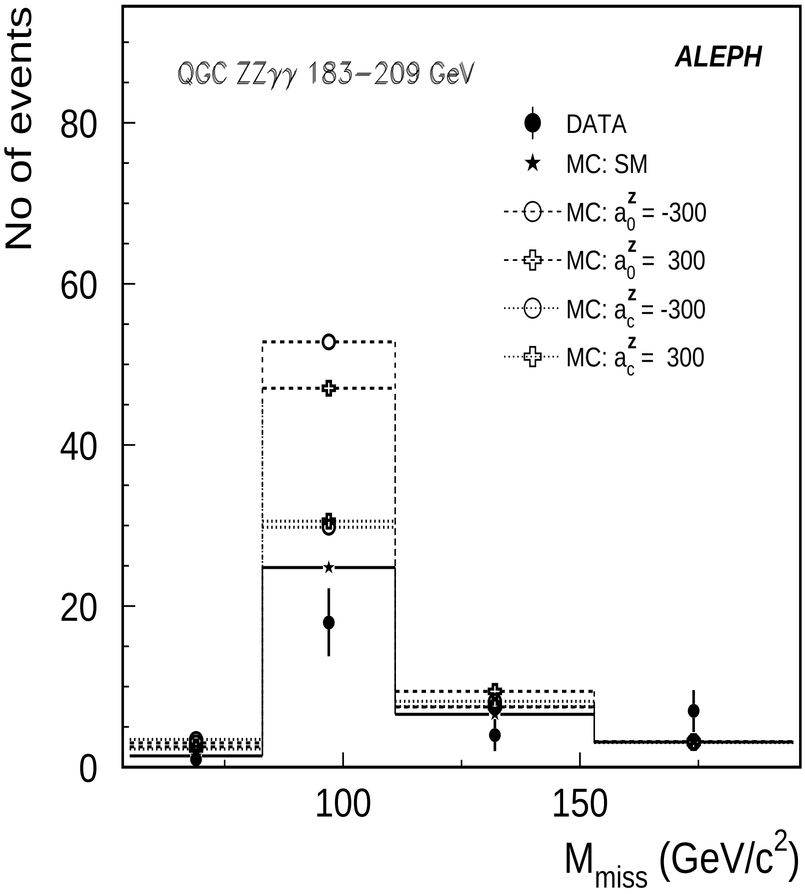

Figure 2: *Missing mass distribution of acoplanar photon pairs selected as described in Section 2.3. Dots with error bars are the data. Other symbols and lines show the predictions from the NUNUGPV Monte Carlo program for different values of the anomalous couplings* a_0^z *and* a_c^z*. The new physics scale* Λ *is set to the mass of the W boson.*

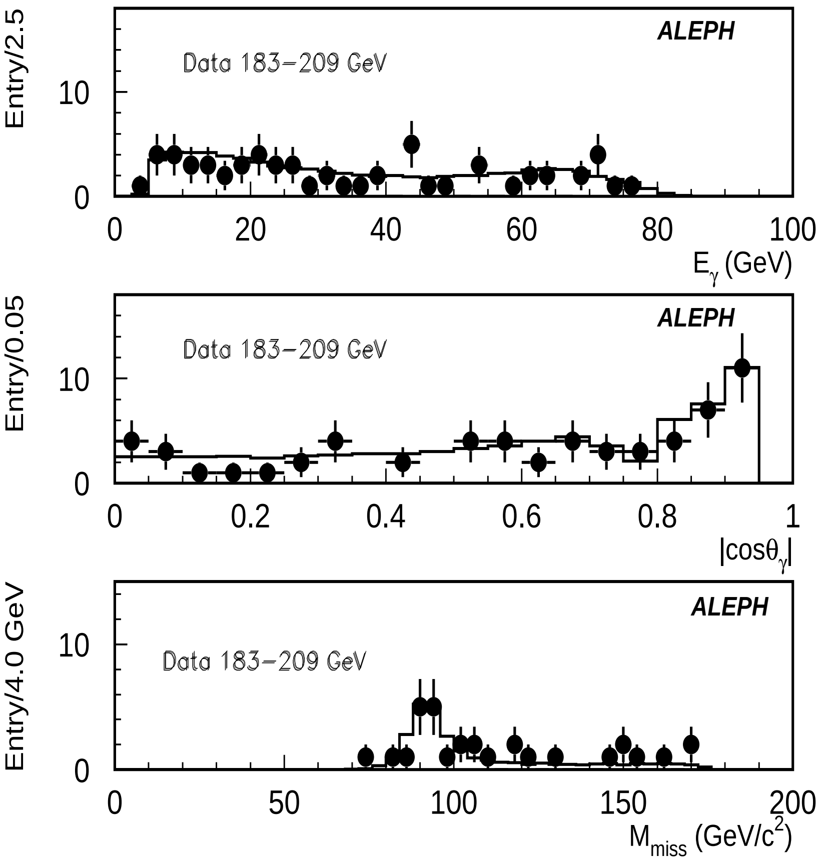

Figure 3: *Distribution of the photon energy E_γ, of $|\cos\theta_\gamma|$ and of the missing mass for the 30 events with two photons selected as described in the text (black dots). The histograms show the SM Monte Carlo predictions corresponding to the total luminosity of the experiment.*

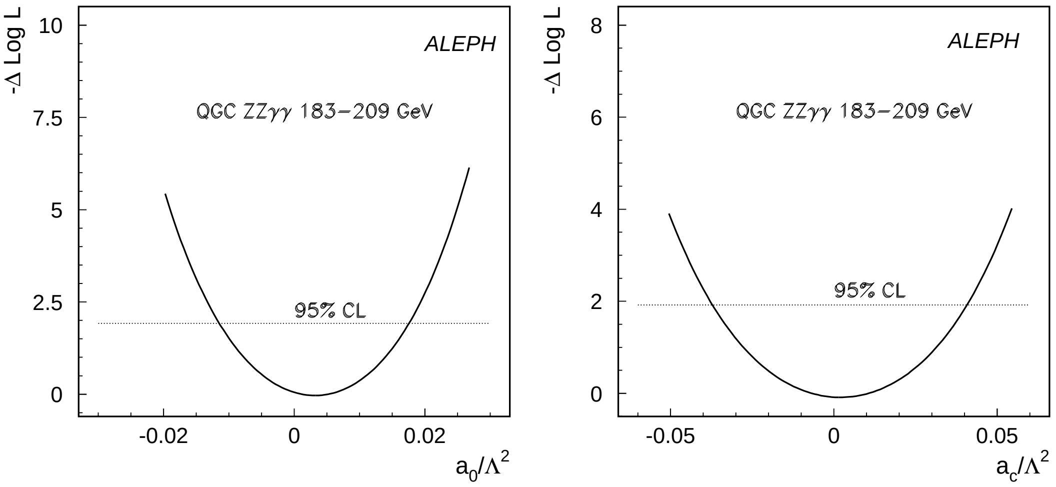

Figure 4: *Likelihood curves for a) the fit of the QGC parameter* $a_0^{\mathrm{Z}}/\Lambda^2$*, the parameter* a_c^{Z} *being set to 0, and b) the fit of* $a_c^{\mathrm{Z}}/\Lambda^2$ *with* a_0^{Z} *set to 0.*

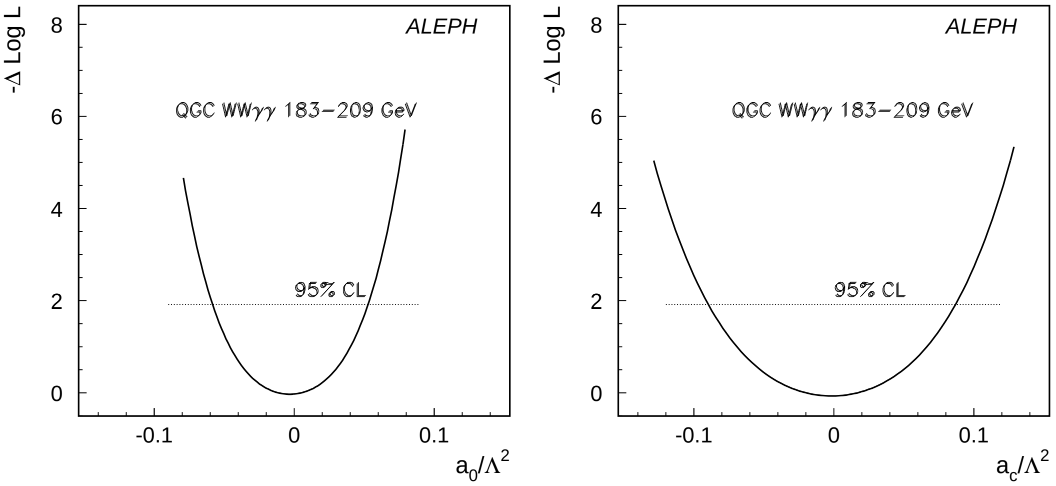

Figure 5: *Likelihood curves for a) the fit of the QGC parameter* $a_0^{\mathrm{W}}/\Lambda^2$*, the parameter* a_c^{W} *being set to 0, and b) the fit of* $a_c^{\mathrm{W}}/\Lambda^2$ *with* a_0^{W} *set to 0.*

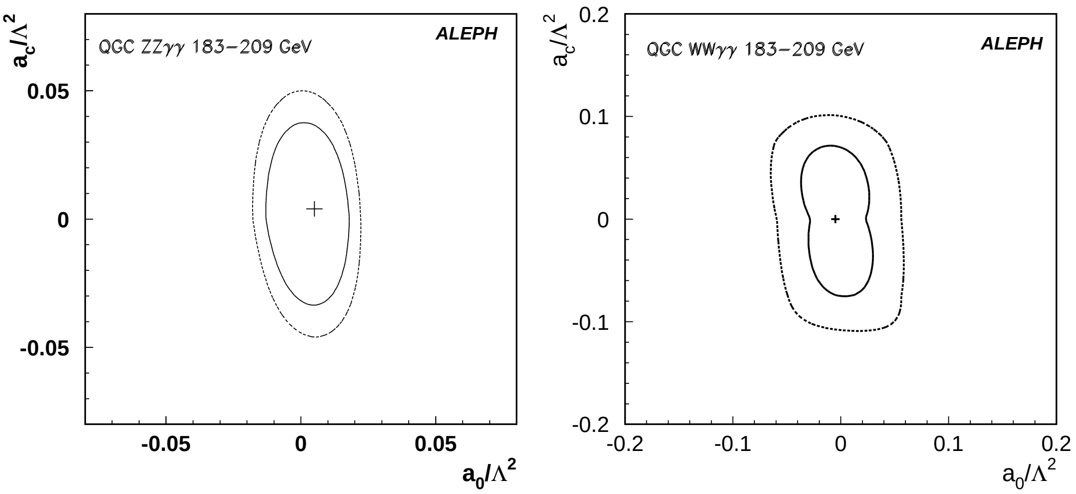

Figure 6: *Two-dimensional contours for the QGC parameters: a)* $a_0^{\rm Z}/\Lambda^2$ *and* $a_{\rm c}^{\rm Z}/\Lambda^2$ *and b)* $a_0^{\rm W}/\Lambda^2$ *and* $a_{\rm c}^{\rm W}/\Lambda^2$*. Full line: 68 % C.L. contour. Dashed line: 95 % C.L. contour.*